Small Rings. Part 32.† The Gas Phase Kinetics, Mechanism, and Energy Hypersurface for the Thermolyses of *syn*- and *anti*-Tricyclo[4.2.0.0^{2,5}]-octane

By **Robin Walsh,*** Department of Chemistry, University of Reading, Whiteknights, Reading RG6 2AD
Hans-Dieter Martin,* Michael Kunze, and **Alfred Oftring,** Institut für Organische Chemie der Universität, D–87, Würzburg, Am Hubland, W. Germany
Hans-Dieter Beckhaus, Chemisches Laboratium der Universität, D-78 Freiburg, Albertstrasse 21, W. Germany

The title reactions have been studied at low pressure (1—10 Torr ‡) and in the temperature ranges 390—419 {*syn*-tricyclo[4.2.0.0^{2,5}]octane (*syn*-TCO)} and 412—445 K (*anti*-TCO). The major products from both compounds were *cis,cis*- and *cis,trans*-cyclo-octa-1,5-diene (*cc*COD and *ct*COD) and, in addition, *anti*-TCO was formed from *syn*-TCO. Minor products from both compounds were *cis*- and *trans*-1,2-divinylcyclobutane (*c*DVC and *t*DVC) and 4-vinylcyclohexene (VCH). The disappearance of the reactant cyclo-octanes followed clear first-order kinetics (independent of pressure) with the rate constants given by equation (i) and (ii) where θ = $RT\ln 10$.§ Both reaction systems were subjected to kinetic analyses which allow for known interconversion pathways amongst the products. These analyses support a mechanism in which the bicyclo[4.2.0]octane-2,5-diyl diradical is a key intermediate. This diradical decomposes to form *ct*COD, *c*DVC, and *cc*COD in the approximate proportions of 60, 15, and 25%. The full mechanism is discussed in terms of a likely potential energy hypersurface for C_8H_{12} hydrocarbons. Combustion calorimetry has been used to arrive at ΔH°_f(l) values for both *syn*- and *anti*-TCO.

$$\textit{syn}\text{-TCO log } k/s^{-1} = (13.37 \pm 0.40) - (31.39 \pm 0.74 \text{ kcal mol}^{-1})/\theta \quad \text{(i)}$$

$$\textit{anti}\text{-TCO log } k/s^{-1} = (14.69 \pm 0.02) - (35.58 \pm 0.04 \text{ kcal mol}^{-1})/\theta \quad \text{(ii)}$$

THE mechanistic interpretation of thermal rearrangements of small strained ring organic molecules offers a continuing challenge, despite extensive study in recent years.[1] The thermochemical kinetic approach of Benson and his co-workers [2] has allowed an enormous body of kinetic information to be systematised and rationalised. This has been particularly fruitful in the area of small ring compound decompositions.[3] The prototype molecules cyclopropane and cyclobutane have been well studied and so in recent years attention has turned, amongst other things, to polycyclic molecules containing these rings.[4,5] Here, with larger molecules, mechanistic complexity inevitably increases. Thermochemical kinetics is not enough in many cases to provide a complete kinetic framework. This is because it is not easy to estimate activation energies for processes which are under orbital symmetry control. Thermal isomerisation and decomposition studies of organic compounds have thrown up many examples of such processes since their importance was first recognised by Woodward and Hoffman [6] a decade ago.

Investigation of *syn*- and *anti*-tricyclo[4.2.0.0^{2,5}]octane (*syn*- and *anti*-TCO) offers the opportunity to probe further some of these considerations. Two of us have recently proposed [7,8] that both *syn*- and *anti*-TCO rearrange *via* the bicyclo[4.2.0]octane-2,5-diyl diradical (with three different conformers) which parallels the tetramethylene diradical intermediate proposed for cyclobutane decomposition. It is also known that the products of this reaction include the interesting strained ring *cis,trans*-cyclo-octa-1,5-diene (*ct*COD), which is itself not particularly stable.[9] It was with a view to obtaining more quantitative information on this system that the present kinetic and calorimetric work was undertaken.

EXPERIMENTAL

(a) *Kinetic Studies.—Apparatus and product analysis.* Experiments were carried out in a conventional high vacuum static pyrolysis system with greaseless Teflon–glass stopcocks and an oil-bath thermostat, whose temperature was controlled to ±0.1%. The handling line and product sample transfer bulbs were all heated to *ca.* 50 °C to minimise handling losses of the tricyclo-octanes by adsorption. Most runs were carried out in a cylindrical reaction vessel of volume *ca.* 100 cm^3 and surface-to-volume ratio of 1.06 cm^{-1}; to test for surface activity a packed vessel of surface-to-volume ratio of 8.07 cm^{-1} was used. Both vessels were conditioned prior to use by three exposures to hexamethyldisilazane. Prior to the study of each compound a test of the system was made by pyrolysing cyclobutene. Rate constants were obtained which fitted the Arrhenius equation, log (k/s^{-1}) = 13.1 − 32.6 kcal mol^{-1}/θ, in good agreement with the known [10] equation (log (k/s^{-1}) = 13.3 − 32.7 kcal mol^{-1}/θ). In the TCO pyrolyses, initial pressures of 7 (*anti*-TCO) and 4 Torr (*syn*-TCO) were normally employed but a few runs were carried out at other pressures in the range 1—10 Torr.

Product analyses were carried out by g.l.c. (Perkin-Elmer F.22) using a 2 m × 3 mm column of OV17 (3% on Chromosorb P) operated at 90 °C with a carrier gas pressure of 1.2 bar. Under these conditions retention times (in min) for observed products were as follows: *trans*-1,2-divinylcyclobutane (*t*DVC), 2.3; *c*DVC, 2.9; 4-vinylcyclohexene (VCH), 3.8; *anti*-TCO, 5.2; *ct*COD, 6.6; *cc*COD, 8.8; *syn*-TCO, 9.7.

† Part 31, H.-D. Martin and B. Mayer, *Tetrahedron Lett.*, 1979, 2351.
‡ 1 Torr = 133.2 N m^{-2}.
§ 1 cal = 4.184 J.

Flame ionisation detection was employed with electronic peak integration (HP 3374 B). For most runs two analyses were carried out and the product percentages averaged. However, persistent difficulties were experienced in handling *ct*COD, because of its instability. Despite attempts to condition handling vessels and the gas sample loop, occasional runs gave irreproducible analyses. Owing to time limitations these could not all be repeated. About 80% of the runs gave reproducible *ct*COD analyses and *ca.* 20% not. In the latter cases the figures for *ct*COD were obtained by back extrapolation from the time of analysis to the time of sampling. This gives rise to some scatter in the *ct*COD results but it was apparent that the sum of *ct*COD and *cc*COD was always reliable (within ±1%). This means that while overall decomposition results were reliable, the relative product pathways were somewhat less so.

(b) *Combustion Calorimetry.—Apparatus and procedure.* Experimental procedures involving the isoperibolic stirred-liquid calorimeter have been described previously.[11] The temperature was measured by a quartz-thermometer (Hewlett–Packard HP2804A). A desk-top computer (Hewlett–Packard HP9815A) was used to start the ignition (u_{ign} 0.52 cal) automatically, and perform all calculations to process the calorimetric data.[12] A set of 6—8 calibration runs with benzoic acid (National Bureau of Standards sample 39i) was interspersed within the series of runs.

The steel bomb (internal volume 0.3004 dm^3) equipped with a platinum crucible (12.8 g) was flushed and charged to 30.00 atm (25.0 °C) with ultrahigh-purity O_2. After this procedure the bomb contained $m^l(H_2O)$ 0.98 g.

The volatile compounds were sealed in small terephthalic acid polyester (Mylar; duPont) bags by soldering iron, to avoid touching the film. Because the film is slightly hygroscopic its weight was corrected [13] *via* m (dry) = $m[1 - 4.6_2 \times 10^{-5} \times$ (relative humidity in %)].

The addition of benzoic acid (runs 2—8) prevented the formation of unburned carbon (soot). No HNO_3 was detected.

Auxiliary quantities and units of measurement. All data reported are based on the 1976 IUPAC atomic weights [14a] and fundamental constants.[14b] For use in reducing weights in air to *in vacuo*, in correcting the energy of the actual bomb process to the isothermal bomb process and in correcting to standard states the following values were used [13] (estimated values are in parentheses). The specific energy of combustion of the auxiliary compounds was measured in preceding experiments:

Polyester film ($C_{10}H_8O_4$), $\Delta u_C°/M$ −5479.7 ± 1.7 cal g^{-1}, ρ 1.38 g cm^{-3}, c_p 0.315 cal g^{-1} K^{-1}, $(\partial V/\partial T)_p$ 10^{-7} K^{-1}

fuse ($C_{1.0}H_{1.774}O_{0.887}$), $\Delta u_C°/M$ −4050.0 ± 4.8 cal g^{-1}, ρ 1.5 g cm^{-3}, c_p 0.4 cal g^{-1}K^{-1}, $(\partial V/\partial T)_p$ 10^{-6} K^{-1}

syn- and *anti*-TCO (C_8H_{12}), ρ (0.86) g cm^{-3}, c_p (0.44) cal g^{-1} K^{-1}, $(\partial V/\partial T)_p$ (8.5 × 10^{-7}) K^{-1}

(c) *Materials.*—The synthesis of the tricyclo-octanes was carried out following literature procedures.[7,15,16] The corresponding tricyclo-octadienes were prepared by sodium and lithium amalgam reduction of 2,3-dichlorocyclobutene. The tricyclo-octadienes were then reduced with potassium azodicarboxylate in methanol giving the mixture of *syn*- and *anti*-TCO. These were separated and purified by g.l.c.

RESULTS

Kinetic Studies

For convenience the decompositions of the two stereoisomeric reactants are treated separately. The analysis of results for the *syn*-compound depends to some extent on that for the *anti*- which is, therefore, taken first.

(A) anti-*TCO.*—(i) *Reactant decomposition.* The observed products, identified and characterised by g.l.c. are listed in the Experimental section. Before anything more complicated was attempted, the reactant decomposition was tested for first-order behaviour. Good linear plots of ln (% *anti*-TCO) against time were obtained, for conversions of up to 90%, for five temperatures in the range 412—445 K. The rate constants obtained together with their standard deviations are shown in Table 1. These constants were

TABLE 1

T/K	412.5	420.5	430.9	440.0	415.1
10^4 k/s^{-1}	0.685 ±0.025	1.563 ±0.051	4.38 ±0.05	10.37 ±0.19	16.44 ±0.19

independent of pressure in the range 1—10 Torr. A further set of runs in the packed vessel at 430.9 K gave k 4.16 × 10^{-4} s^{-1}, a value in sufficiently close agreement with the unpacked vessel figure to remove any suspicion of a heterogeneous process. An Arrhenius plot of the constants in Table 1 gave $\log(k/s^{-1}) = (14.69 \pm 0.02) - (35.58 \pm 0.04)/\theta$ where the error limits correspond to one standard deviation (68% confidence level). The Arrhenius data correspond to activation parameters of $\Delta S^‡$ +6.0 cal K^{-1} mol^{-1} and $\Delta H^‡$ 34.7 kcal mol^{-1}.

(ii) *Detailed kinetic fit.* Figure 1 shows the time evolution

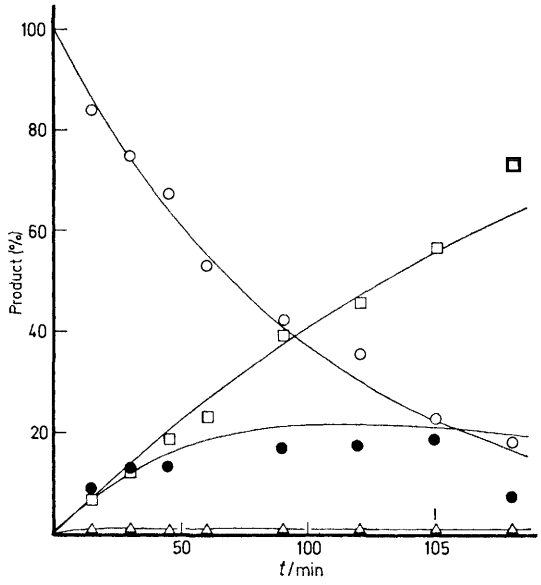

FIGURE 1 Product percentage time evolution for *anti*-TCO at 420.5 K (*anti*-TCO, ○; *ct*COD, ●; *cc*COD, □; *c*DVC, △)

of the products in a typical series of runs at 420.5 K. The major product behaviour can be seen clearly but of the minor products only *c*DVC is shown for convenience. *c*DVC differs from the other minor products in that it tends to reach a steady state (in this case 0.7 ± 0.1%) and stay approximately constant during the reaction. *t*DVC (0.2% after 180 min) and VCH (*ca.* 0.8% after 180 min) on the other hand tended to build up slowly during the reaction.

This suggests that *c*DVC (as well as *ct*COD) is an intermediate in this system. It is, of course, known from independent studies that both *ct*COD [9] and *c*DVC [17] are labile under the conditions of these experiments. Scheme 1

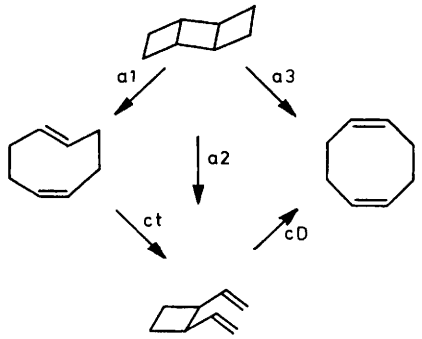

SCHEME 1

incorporates the known and proposed unimolecular processes occurring in this system. In this scheme it is assumed, as recently suggested,[9] that *ct*COD isomerisation proceeds *via* *c*DVC to *cc*COD and not directly. The minor return process of *c*DVC to *ct*COD is neglected. The fact that *c*DVC is only observed at a low level in this system is the result of its fast process (high k_{cD} value) to *cc*COD. It should be emphasised that pathways from *anti*-TCO to all other three components of Scheme 1 must be included (as the results will bear out). The minor products *t*DVC and VCH are, however, sufficiently unimportant to justify their neglect.

For convenience of treatment the analysis of this scheme is sub-divided into two stages, (a) a simplified scheme (Scheme 2) with only three rate constants which neglects the presence of *c*DVC and (b) the full scheme with five rate constants.

(a) Three rate constant scheme (Scheme 2). The simplification of treatment assumed here is justified by the fact that *c*DVC is at the level of $\leqslant 1\%$ and thus any *cc*COD formed *via* *c*DVC can be assumed to depend on rate-determining formation of *c*DVC. Hence the relationship between the rate constants for Schemes 2 and 1.

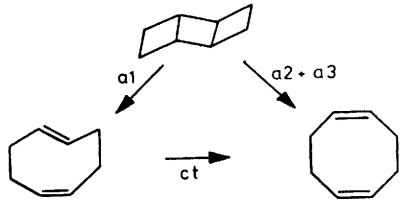

SCHEME 2

The major products at each temperature were, therefore, fitted to Scheme 2 using a computer-controlled optimisation routine which adjusted rate constant values in order to minimise the squares of percentage deviations of experimental from calculated product percentage.[18] The calculated product percentages were obtained using the standard analytical expressions for such a three rate constant scheme (see Appendix). In a trial attempt with no constraints on the rate constants values were obtained which varied very erratically with temperature. This arose because of the somewhat scattered percentage figures for *ct*COD (see Experimental section). Much less erratic figures were obtained when k_{ct} was kept fixed by use of values calculated from our previous independent study.[9] These latter figures are listed in Table 2. A glance at Table 2 shows that *ct*COD formation represents *ca.* 50%

TABLE 2

Rate constants ($10^4\ k/s^{-1}$) for Scheme 2

T/K	k_{a1}	$k_{a2} + k_{a3}$	k_{ct}*
412.5	0.399	0.300	0.588
420.5	0.862	0.786	1.237
430.9	2.17	2.19	3.14
440.0	4.87	5.23	6.78

* Calculated from [9] $\log (k_{ct}/s^{-1}) = 12.77 - 32.08\ \text{kcal mol}^{-1}/\theta$.

(temperature dependent) of the primary product of reaction.

(b) Five rate constant scheme (Scheme 1). The above analysis was now extended by making use of the steady state concentrations of *c*DVC, given by equation (1). Both

$$k_{cD}[c\text{DVC}] = k_{a2}[anti\text{-TCO}] + k_{ct}[ct\text{COD}] \qquad (1)$$

k_{cD} [$\log (k_{cD}/s^{-1}) = 10.81 - 25.33/\theta$] and k_{ct} (see Table 2) were available from our previous study of *ct*COD isomerisation and thus k_{a2} is the only unknown rate constant in this relationship. Values were calculated from the measured concentrations for each analytical run and averaged for each temperature. Because of the low concentration of *c*DVC the uncertainty in each value is probable *ca.* $\pm 20\%$. The results are shown in Table 3

TABLE 3

Rate constants ($10^4 k/s^{-1}$) for steps a2 and a3 (Scheme 1)

T/K	k_{a2}	k_{a3}
412.5	0.11	0.19
420.5	0.19	0.58
430.9	0.76	1.4
440.0	2.2	3.1

which also includes k_{a3} obtained by subtraction of k_{a2} values from $k_{a2} + k_{a3}$ (Table 2). Despite the admitted uncertainties it is quite clear from these figures that a substantial portion of *cc*COD comes *via* the intermediacy of *c*DVC.

In summary this treatment of the detailed product analyses has provided values for k_{a1}, k_{a2}, and k_{a3} at four temperatures for which analytical data were available. The precision of the figures is not judged to be sufficient to warrant presentation of Arrhenius parameters. Instead we show in Table 4 the percentages of *anti*-TCO which react

TABLE 4

Percentage distribution of *anti*-TCO decomposition pathways

T/K	a1	a2	a3
412.5	57.1	15.9	27.0
420.5	52.3	11.6	35.0
430.9	49.9	17.4	32.7
440.0	48.2	21.4	30.4
Average	51.9	16.6	31.3

via the three pathways. The figures justify the assumption that all three pathways are important and indicate the important role played by *c*DVC in this decomposition. For the purposes of the discussion, average figures are also shown.

(B) syn-*TCO*.—(i) *Reactant decomposition.* In addition

to all the products observed for the *anti*-TCO decomposition, *anti*-TCO itself was formed from *syn*-TCO. Prior to detailed analysis of individual yields, the reactant decomposition was tested for first-order behaviour. Good linear plots of ln(% *syn*-TCO) against time were obtained for conversions up to 90%, for eight temperatures in the range 390—418 K. The rate constants obtained together with their standard deviations are shown in Table 5. These

TABLE 5

T/K	390.2	395.8	399.6	404.1	408.5
10^4k/s^{-1}	0.557 ±0.033	1.107 ±0.049	1.559 ±0.065	2.42 ±0.11	3.86 ±0.16
T/K	411.3	415.5	418.4		
10^4k/s^{-1}	5.04 ±0.15	7.08 ±0.22	8.36 ±0.51		

constants were independent of pressure in the range 1—10 Torr. A further set of runs in the packed vessel at 411.3 K gave k 4.58 × 10^{-4} s^{-1}, a value in sufficiently close agreement with the unpacked vessel figure to remove any suspicion of a heterogeneous process. An Arrhenius plot of the constants in Table 5 gave log $(k/s^{-1}) = (13.37 \pm 0.40) - (31.39 \pm 0.74)/\theta$ where the error limits correspond to one standard deviation (68% confidence level). The Arrhenius data correspond to activation parameters of $\Delta S^{\ddagger}$ 0.0 cal K^{-1} mol^{-1} and $\Delta H^{\ddagger}$ 30.6 kcal mol^{-1}. It is worth noting that *syn*-TCO decomposes about eight times faster than *anti*-TCO at the temperatures of these studies.

(ii) *Detailed kinetic fit.* Figure 2 shows the time evolution

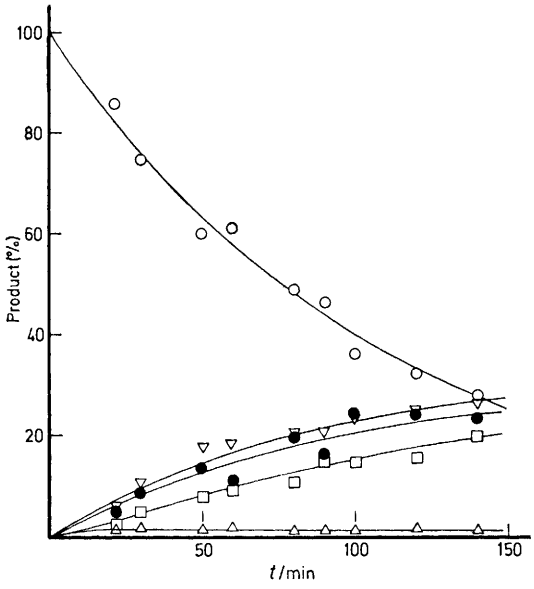

FIGURE 2 Product percentage time evolution for *syn*-TCO at 399.6 K (*syn*-TCO, ○; *anti*-TCO, ▽; *ct*COD ●; *cc*COD □; *c*DVC, △)

of the products in a typical series of runs at 399.6 K. *anti*-TCO is marginally the most important product, but the *syn*-TCO decomposition is sufficiently fast that the *anti*-TCO and *ct*COD yields do not reach the maxima characteristic of intermediates within the time scale of this run. Nevertheless from their independently measured decomposition rates we know that some secondary reaction is taking place. Once again *c*DVC only of the minor products is shown. It again shows the characteristic steady state level (1.2 ± 0.3%) of an intermediate while *t*DVC (0.2% after 140 min) and VCH (0.3% after 140 min) tend to build up slowly during the reaction. Scheme 3 incorporates the

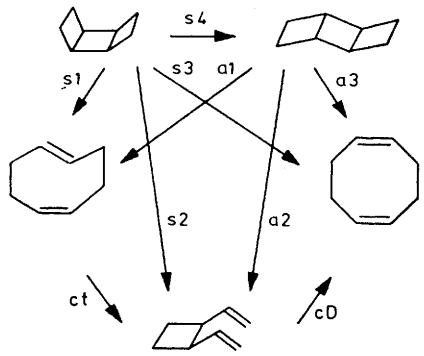

SCHEME 3

known and proposed unimolecular processes occurring in this system. This Scheme is an amplification of Scheme 1, in which, in addition to all the processes proposed for *anti*-TCO decomposition, four additional pathways are included to allow for the possibility that all four products may arise directly from *syn*-TCO. It is again worth stressing that the minor product *c*DVC, is an important intermediate, while the other minor products, which are therefore neglected, are not so.

For the sake of convenience of treatment once again the modelling of this scheme is divided into two stages (a) a simplified Scheme 4 with only six rate constants which neglects the presence of *c*DVC and (b) the full Scheme 3 with nine rate constants.

(a) Six rate constant scheme (Scheme 4). As in the case

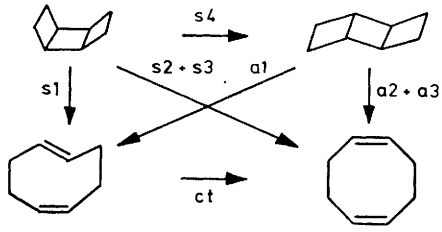

SCHEME 4

of *anti*-TCO, the simplified scheme is justified on the grounds that *c*DVC is at such a low level that any *cc*COD formed *via* its intermediacy can be assumed to depend only on the rate of formation of *c*DVC. Hence the relationship between the rate constants for Schemes 3 and 4. The major product data at each temperature were therefore first fitted to Scheme 4. Although unimolecular rate networks can be solved by general methods, this particular scheme has an analytical solution which is more easily handled (see Appendix). To avoid ambiguities in the solution, three quantities were regarded as fixed whilst three were allowed to vary. This was facilitated by our prior knowledge of the *anti*-TCO and *ct*COD decompositions. Thus the fixed quantities were the sum $k_{a1} + k_{a2} + k_{a3}$, the constant k_{ct}, and the relationship $k_{s1}/(k_{s2} + k_{s3}) = k_{a1}/(k_{a2} + k_{a3})$. The values for $k_{a1} + k_{a2} + k_{a3}$ and for k_{ct} were calculated from the appropriate Arrhenius equations [see Results (A)

and ref. 9]. The solutions obtained were fairly insensitive to these particular constants and, therefore, any error in these values was not serious. The relationship $k_{s1}/(k_{s2} + k_{s3}) = k_{a1}/(k_{a2} + k_{a3})$ is equivalent to the statement that the ratio [*ct*COD] : [*cc*COD] should be the same starting from either *syn*- or *anti*-TCO. This seemed reasonable *a priori* (however see below).

The results are summarised in Table 6 which simply

TABLE 6

Rate constants ($10^4k/s^{-1}$) for Scheme 4

T/K	k_{s1}	$k_{s2} + k_{s3}$	k_{s4}
395.8	0.411	0.245	0.452
399.6	0.535	0.371	0.624
404.1	0.970	0.552	1.002
408.5	1.492	0.781	1.667
411.3	1.718	1.215	2.11
415.5	2.73	1.705	2.98
418.4	3.40	1.799	3.75

shows the three derived, best-fit constants, not the fixed quantities, at each temperature. As a check, the sum $k_{s1} + k_{s2} + k_{s3} + k_{s4}$ was compared to the total decomposition constant at each temperature and found to be within a few per cent in every case. The Arrhenius equation, $\log(k_{s1} + k_{s2} + k_{s3} + k_{s4}) = 13.31 - 31.27/\theta$ may be derived from Table 6. It is worth noting that the principal pathway is *anti*-TCO formation and also that *ct*COD exceeds *cc*COD formation.

(b) Nine rate constant scheme (Scheme 3). The above analysis was now extended (as with *anti*-TCO) to take account of the steady state concentrations of *c*DVC. These are given by equation (2). Both k_{cD} and k_{ct} are known

$$k_{cD}[cDVC] = k_{s2}[syn\text{-TCO}] + k_{a2}[anti\text{-TCO}] + k_{ct}[ctCOD] \quad (2)$$

[see Results (A)] and k_{a2} was calculated from $\log(k_{a2}/s^{-1}) = 14.70 - 37.12/\theta$ (a preferred fit equation to the data of Table 3). Thus k_{s2} is the only unknown rate constant in this relationship. Values were calculated from the measured concentrations for each analytical run and averaged for each temperature. Once again because of the low concentration of *c*DVC the uncertainty in each value is probably ± 20%. The results are shown in Table 7 which also includes k_{s3} obtained by subtraction of k_{s2} from $k_{s2} + k_{s3}$ (Table 6). Despite the admitted uncertainties it is quite clear from these figures that once again a substantial portion of the *cc*COD comes *via* the intermediacy of *c*DVC.

TABLE 7

Rate constants ($10^4k/s^{-1}$) for steps s2 and s3 (Scheme 3)

T/K	k_{s2}	k_{s3}
395.8	0.095	0.15
399.6	0.14	0.23
404.1	0.23	0.33
408.5	0.31	0.48
411.3	0.37	0.84
415.5	0.53	1.18
418.4	0.66	1.14

In summary, this kinetic treatment of the *syn*-TCO decomposition has provided values for k_{s1}, k_{s2}, k_{s3}, and k_{s4} at seven temperatures for which analytical data were available. The precision of the figures is not judged to be sufficient to warrant presentation of Arrhenius parameters. Instead we show in Table 8 the percentages of *syn*-TCO which react *via* the four possible pathways. The figures clearly justify the assumption that all four pathways are important and show yet again the important role played by *c*DVC in this decomposition. Also included in Table 8 are percentages (in parentheses) based only on processes s1—s3 (*i.e.* neglecting s4) for purposes of comparison with

TABLE 8

Percentage distribution of *syn*-TCO decomposition pathways

T/K	s1	s2	s3	s4
395.8	37.1 (62.7)	8.6 (14.5)	13.5 (22.9)	40.8
399.6	35.0 (59.1)	9.1 (15.3)	15.2 (25.6)	40.8
404.1	38.3 (63.5)	8.9 (14.8)	12.9 (21.3)	39.6
408.5	37.9 (65.6)	7.8 (13.5)	12.1 (20.9)	42.3
411.3	34.1 (58.6)	7.4 (12.7)	16.7 (28.8)	41.9
415.5	36.8 (61.5)	7.1 (11.9)	15.9 (26.6)	40.2
418.4	38.0 (65.4)	7.4 (12.8)	12.7 (21.9)	41.9
Average	36.7 (62.3)	8.0 (13.6)	14.1 (24.0)	41.1

Table 4. Apparently the relative probabilities of decomposition from *syn*-TCO vary little with temperature, while those from *anti*-TCO vary somewhat more. We suspect a source of error in the *anti*-TCO values (see Discussion). It should be noted that, in deriving the *syn*-TCO values, these relative probabilities were assumed the same (at a given temperature). However, the values for the *syn*-TCO rate constants are insensitive to small variations in the *anti*-TCO rate constants, and, therefore, the *syn*-TCO values may be regarded as independent of this assumption.

Calorimetric Studies

The combustion results are presented in standard form in Table 9. The standard combustion enthalpies were converted into the enthalpies of formation shown in Table 10.

TABLE 9

Summary of calorimetric experiments at 298.15 K[a]

	syn-TCO					*anti*-TCO		
	1	2	3	4	5	6	7	8
m' (compound)/g	0.207 85	0.169 38	0.195 92	0.189 15	0.228 98	0.196 91	0.230 31	0.224 13
m''(polyester)/g [b]	0.028 40	0.019 41	0.018 91	0.020 96	0.020 68	0.016 98	0.023 57	0.022 1
m'''(fuse)/g	0.001 00	0.001 00	0.001 25	0.001 00	0.001 00	0.001 18	0.001 22	0.001 22
m''''(benzoic acid)/g	—	0.391 11	0.388 82	0.396 81	0.384 55	0.390 20	0.372 36	0.327 37
Δt_c/K [c]	1.110 09	2.015 78	2.139 03	2.135 45	2.297 77	2.139 96	2.272 83	2.236 96
ϵ(calor)$(-\Delta t_c)$/cal [d]	2 463.0	4 467.6	4 740.7	4 732.8	5 092.6	4 743.2	5 037.7	4 958.2
ϵ(cont.)(Δt_c)/cal [e]	5.14	7.46	8.00	7.98	8.57	7.92	8.48	8.34
Δu (correction to standard states)/cal. [f]	0.90	2.66	2.77	2.79	2.91	2.77	2.87	2.83
$-(m''\Delta u°_C/M)$(polyester)/cal	155.33	106.38	103.44	114.87	113.31	93.03	129.15	121.54
$-(m'''\Delta u°_C/M)$(fuse)/cal	4.05	4.05	5.07	4.05	4.05	4.78	4.62	4.94
$-(m''''\Delta u°_C/M)$(benzoic acid)/cal	—	2 469.0	2 454.5	2 505.0	2 427.6	2 463.2	2 350.6	2 350.7
$\Delta u°_C$ (unburned C)/cal. [g]	8.31	—	—	—	—	—	—	—
$\Delta u°_C/M$ (compound)/cal g^{-1}	−11 141	−11 173	−11 139	−11 174	−11 148	−11 105	−11 108	−11 092
$\Delta H°_C$ (compound)/kcal mol^{-1}	− 1206.9	−1 210.4	−1 206.8	−1 210.5	−1 207.7e	−1 203.1	−1 203.4	−1 201.6

[a] The symbols used are those of ref. 12, except that internal energy is represented by u. [b] Corrected to relative humidity of 0%, see ref. 13. [c] $\Delta t_c = t_f - t_i - \Delta t_{corr.}$ [d] ϵ (calor) = 2 218.7 ± 0.3 (run 1), 2 216.3 ± 0.6 (run 2—5), 2 216.5 ± 0.5 (run 6—8). [e] ϵ_i (cont.)$(t_i - 298.15) + \epsilon_f$ (cont.)$(298.15 - t_f + \Delta t_{corr.})$. [f] Items 81—85, 87—90, and 94 of the computation form of ref. 12. [g] Correction for unburned carbon (soot), at 7 900 cal. g^{-1}.

TABLE 10

Enthalpies of combustion and formation of *syn*- and *anti*-TCO at 298.15 K in kcal mol^{-1} [a]

	$\Delta H°_c$ (l)	$\Delta H°_f$ (l)	$\Delta H°_f$ (g) [b]
syn-TCO	−1 208.5 ± 0.9	46.2 ± 0.9	56.2 ± 1.0
anti-TCO	−1 202.7 ± 0.6	40.4 ± 0.6	50.4 ± 0.7
Difference	5.8 ± 1.1		5.8 ± 1.2

[a] The given standard deviation of the mean includes the uncertainties of calibration experiments and those of the enthalpies of combustion of all auxiliary compounds. [b] The heats of vaporization of both *syn*- and *anti*-TCO have been approximated as 10.0 ± 0.4 kcal mol^{-1} based on the values ($\Delta H°_v$/kcal mol^{-1}): cyclo-octane, 10.3; bicyclo[5.1.0]octane, 10.4; cyclo-octatetraene, 10.3, bicyclo[4.2.0]octane, 9.8 (J. D. Cox and G. Pilcher, ' Thermochemistry of Organic and Organometallic Compounds,' Academic Press, London, 1970).

Gas-phase values have been obtained by use of reasonable estimates of vaporisation enthalpies. There is a clearly discernible difference between the values for the two TCO isomers.

DISCUSSION

(1) *Overall Decomposition of Tricyclo-octanes.*—There has been no previous kinetic investigation of the tricyclo-octanes. The Arrhenius parameters for their decompositions are compared with those for cyclobutane and for bicyclo[2.2.0]hexane in Table 11. It

TABLE 11

Arrhenius parameters for fused ring cyclobutane thermolyses

Reactant	log A/s^{-1}	E_a/kcal mol^{-1}	Reference
Cyclobutane	15.6	62.5	*a*
Bicyclo[2.2.0]hexane	13.4	36.0	*b*
anti-TCO	14.7	35.6	This work
syn-TCO	13.4	31.4	This work

[a] R. W. Carr, jun. and W. D. Walters, *J. Phys. Chem.*, 1963, **67**, 1370. [b] C. Steel, R. Zand, P. Hurwitz, and S. G. Cohen, *J. Am. Chem. Soc.*, 1964, **86**, 679.

can be seen that whereas there are significant differences between one four-membered ring (cyclobutane) and two edge fused four-membered rings (bicyclo[2.2.0]hexane), there are only small differences between the latter and the three fused cyclobutane ring case (tricyclo-octanes). This supports the idea of a similar mechanism and energetics for the latter two cases and also that the third cyclobutane ring has little influence at the rate-determining stage of the reaction. Entropies of activation are small, suggesting little, if any, loosening of structure at the transition state. It is doubtful if the small difference between *anti*-TCO ($\Delta S^{\ddagger} = 6.0$ ca lK^{-1} mol^{-1}) and *syn*-TCO ($\Delta S^{\ddagger} = 0$) has any great significance, especially bearing in mind experimental uncertainties. The activation energy for *anti*-TCO is almost identical with that for bicyclo[2.2.0]hexane whilst that for *syn*-TCO is less by a small, but we believe significant, amount, *viz.* 4 kcal mol^{-1}. The most likely explanation for this appears to be a ground-state destabilisation effect due to steric strain which is largely relieved in the transition state for *syn*-TCO isomerisation. The magnitude of this effect 5.8 ± 1.2 kcal mol^{-1} is provided by the observed difference in the heats of formation obtained in this work. An effect of similar magnitude was observed in the thermolysis of *syn*-tricyclo[4.2.0.0^{2,5}]-octa-3,7-diene.[19]

Bicyclo[2.2.0]hexane isomerisation has long been thought to proceed *via* a diradical mechanism [20] (we draw no significant distinction here between Benson's diradicals [21] and Dewar's diradicaloids [22]). Thus these considerations all lend support to our earlier suggested diradical mechanism.[7] This theme is developed further in the next section.

(2) *Detailed Mechanism in Tricyclo-octane Decomposition.*—The kinetic analyses of the product distribution have shown support for the mechanisms represented by Schemes 1(*anti*-TCO) and 3(*syn*-TCO). These

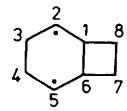

(I)

product distributions fit well the concept of a diradical intermediate. The diradical in question is bicyclo-[4.2.0]octane-2,5-diyl (I). Thus *ct*COD and *cc*COD are produced by 1,6 C–C bond breaking, *c*DVC results from 3,4 C–C bond breaking, and *anti*-TCO from 2,5 C–C recombination. It is possible that *syn*-TCO could also form *via* 2,5 C–C recombination but this could only be observed starting from *anti*-TCO, and since *syn*-TCO decomposes more rapidly than *anti*-TCO this would be difficult to detect. All other possible processes are however observed. It is reasonable that the pathways to the cyclo-octadienes predominate since the 1,6 C–C bond must be significantly weaker than the 3,4 C–C bond. However, the fact that a direct pathway to *c*DVC exists at all indicates that this energetic advantage is far from overwhelming. The division of the cyclo-octadienes into *ct*COD and *cc*COD is governed by conformational preferences in the diradical which can exist in three forms which are probably in rapid mobile equilibrium as shown in Scheme 5. Thus the origin of

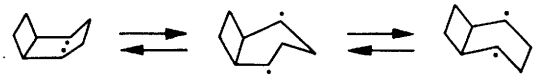

SCHEME 5

the preference for *ct*COD formation lies in the likely preference of the diradical for the quasi-chair form. The preference for single-carbon stereochemical inversion as indicated by *ct*COD predominance seen in this work and previously,[7] is consistent with the finding of predominant formation of *cis,trans*-hexa-1,5-dienes in bicyclo[2.2.0]hexane thermolysis.[23] In principle, with a common diradical intermediate the product distribution from both tricyclo-octanes should be the same (apart from mutual interconversion, see above). Unfortunately the results do not quite bear this out. We feel that this probably arises from the uncertainties associated with

the *ct*COD analysis referred to in the Experimental section. As these were greater in the case of *anti*- than *syn*-TCO it is likely that the pathway (product) distribution figures of Table 8 are probably more reliable than those of Table 4. This is also made more likely by the fact that the figures of Table 8 show a less erratic temperature variation than those of Table 4. The averages at least do not show too great a disparity. It would be nice to analyse the decomposition preferences of diradicals in terms of energy and entropy effects but this would require data of a much higher precision than we have been able to obtain. At least from the *syn*-TCO data there appears to be no evidence of any *strong* temperature dependence of the decomposition distribution and therefore there can be no very large activation energy differences.

These arguments form a self-consistent and satisfying picture of the mechanism of the tricyclo-octane isomerisations but do not, of course, rule out completely the possibility of a partial degree of concertedness in these reactions. A ($_{\sigma}2_s + {}_{\sigma}2_a$) pathway [6,7] would lead to *ct*COD (and also *c*DVC) and this might contribute to the rate. The degree of concertedness in the decompositions of other bicyclic compounds containing cyclobutane rings is, however, known to be small,[24,25] and, as discussed elsewhere,[7] we feel it is likely to be unimportant in the present case. Of more interest in relation to the present work is the study made previously by two of us on the thermal and photochemical decomposition [8] of *anti*-7,8-diazatricyclo[4.2.2.0^{2,5}]dec-7-ene. This azo-compound is a potential alternative precursor to the bicyclo[4.2.0]octane-2,5-diyl diradical and indeed in the photolysis, *ct*COD, *cc*COD, *c*DVC, and *anti*-TCO were all observed. The thermolysis [7,8] is postulated to decompose in large part *via* a concerted pathway to *cc*COD, with a minor diradical pathway to other products. The temperature of study, however, is high (250—290 °C) and the other products are unstable and, therefore, the extent of this other pathway may be significant. In the case of room temperature photolyses [8] in various solvents product percentages were in the ranges *ct*COD 34—71%, *cc*COD 7—37%, *c*DVC 8—12%, and *anti*-TCO 8—41%. The complications of solvent effects and excited state spin and symmetry properties doubtless render any comparison highly speculative, but these percentages are sufficiently close to those of the thermolyses of the tricyclo-octanes at least to suggest some similarities in mechanism.

(3) *Potential Energy Hypersurface for* C_8H_{12} *Hydrocarbons.*—Figure 3 presents such a surface and effectively summarises the energetics of the tricyclo-octane decompositions and those of our related earlier study [9] of *ct*COD. The diradical heats of formation were calculated by the methods of thermochemical kinetics [26] and are found to lie satisfactorily 4—6 kcal mol^{-1} below those of the transition states whose heats of formation are based on the activation enthalpies and heats of formation determined in this work. Other heats of formation were either taken from the literature or estimated.[27—30] This energy surface, of course, only correlates those compounds forming a part of our studies. Further portions of this energy surface for C_8H_{12} hydrocarbons may be found in the work of Doering [31] and Huybrechts.[27]

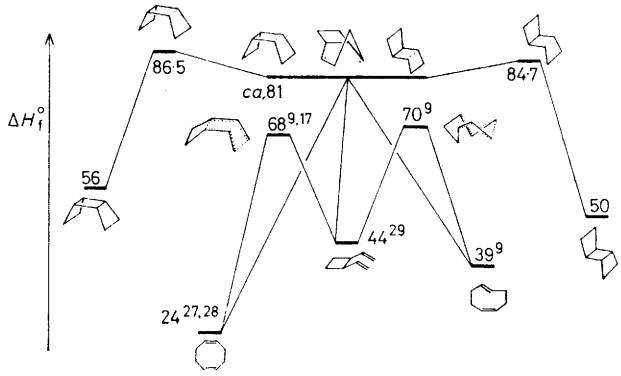

FIGURE 3 Energy (enthalpy) hypersurface for a selection of C_8H_{12} hydrocarbons. Where heats of formation are unreferenced, refer to text

APPENDIX

Published particular solutions to the reactions systems of interest here are peculiarly elusive, although more general solutions are given in various texts.[32,33] For convenience, therefore, analytical solutions are given explicitly here for the relevant cases.

(a) *Solution of the Three Rate Constant Scheme.*—The

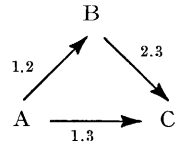

concentration–time dependencies are given by equations (3)—(5).

$$[A] = A_o e^{-\lambda_1 t} \quad (3)$$

where $A_o = [A]$ at $t = 0$ and $\lambda_1 = k_{1.2} + k_{1.3}$.

$$[B] = A_o \frac{k_{1.2}}{k_{2.3} - \lambda_1} (e^{-\lambda_1 t} - e^{-\lambda_2 t}) \quad (4)$$

where $\lambda_2 = k_{2.3}$.

$$[C] = A_o - ([A] + [B]) \quad (5)$$

(b) *Solutions to the Six Rate Constant Scheme.*—The concentration–time dependencies are given by equations (6)—(9).

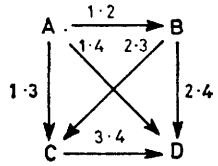

$$[A] = A_o e^{-\lambda_1 t} \quad (6)$$

where $A_o = [A]$ at $t = 0$ and $\lambda_1 = k_{1.2} + k_{1.3} + k_{1.4}$.

$$[B] = A_0 \frac{k_{1.2}}{\lambda_2 - \lambda_1} (e^{-\lambda_1 t} - e^{-\lambda_2 t}) \quad (7)$$

where $\lambda_2 = k_{2.3} + k_{2.4}$.

$$[C] = A_0(Q_{1e}^{-\lambda_1 t} + Q_{2e}^{-\lambda_2 t} + Q_{3e}^{-\lambda_3 t}) \quad (8)$$

where $\lambda_3 = k_{3.4}$, $Q_1 = k_{1\,3}/(\lambda_3 - \lambda_1) + k_{1.2}k_{2.3}/(\lambda_3 - \lambda_1)(\lambda_2 - \lambda_1)$, $Q_2 = -k_{1.2}k_{2.3}/(\lambda_3 - \lambda_2)(\lambda_2 - \lambda_1)$, and $Q_3 = -k_{1.3}/(\lambda_3 - \lambda_1) + k_{1.2}k_{2.3}/(\lambda_3 - \lambda_1)(\lambda_3 - \lambda_2)$.

$$[D] = A_0 - ([A] + [B] + [C]) \quad (9)$$

We thank the Deutsche Forschungs-gemeinschaft, the Fonds der Chemischen Industrie and the BASF AG for financial support. We thank also Professor Doering for sending us his unpublished results on butadiene dimerisation.

[0/896 *Received*, 11*th June*, 1980]

REFERENCES

[1] J. A. Berson, *Ann. Rev. Phys. Chem.*, 1977, **28**, 111.
[2] S. W. Benson, ' Thermochemical Kinetics ', Wiley-Interscience, New York, 1976, 2nd edn.
[3] H. E. O'Neal and S. W. Benson, *J. Phys. Chem.*, 1968, **72**, 1866.
[4] H. E. O'Neal and S. W. Benson, *Int. J. Chem. Kinet.*, 1970, **2**, 423.
[5] For detailed but not exhaustive compilations see Special Periodical Reports of the Chemical Society, vol. 1, 1975 (ed. P. G. Ashmore), P. J. Robinson, p. 23; vol. 3, 1978 (eds. P. G. Ashmore and R. J. Donovan), H. M. Frey and R. Walsh, p. 1.
[6] R. B. Woodward and R. Hoffmann, ' The Conservation of Orbital Symmetry ', Academic Press, New York, 1970.
[7] H.-D. Martin and E. Eisenmann, *Tetrahedron Lett.*, 1975, 661; H.-D. Martin, E. Eisenmann, M. Kunze, and V. Bonačič-Koutecký, *Chem. Ber.*, 1980, **113**, 1153.
[8] H.-D. Martin, B. Heiser, and M. Kunze, *Angew. Chemie. Int. Ed. Engl.*, 1978, **17**, 696; N. J. Turro, J. Liu, H.-D. Martin. and M. Kunze, *Tetrahedron Lett.*, 1980, 1299.
[9] H.-D. Martin, M. Kunze, H.-D. Beckhaus, R. Walsh, and R. Gleiter, *Tetrahedron Lett.*, 1979, 3069; J. Leitich, *Int. J. Chem. Kinet.*, 1979, **11**, 1249.
[10] W. P. Hauser and W. D. Walters, *J. Phys. Chem.*, 1963, **67**, 1328.
[11] H.-D. Beckhaus, G. Kratt, K. Lay, J. Geiselmann, C. Rüchardt, B. Kitschke, and H. J. Lindner, *Chem. Ber.*, 1980, **113**, 3441.
[12] W. N. Hubbard, D. W. Scott, and G. Waddington in ' Experimental Thermochemistry ', ed. F. D. Rossini, Interscience, New York, 1956, p. 75.
[13] W. D. Good, D. R. Douslin, D. W. Scott, A. George, J. L. Lacina, J. P. Dawson, and G. Waddington, *J. Phys. Chem.* 1959, **63**, 1133.
[14] (*a*) IUPAC Commission on Atomic Weights, N. N. Greenwood, *Pure Appl. Chem.*, 1974, **37**, 589; (*b*) F. D. Rossini in ' Combustion Calorimetry ', eds. S. Sunner and M. Månsson, Pergamon, Oxford, 1979, p. 1.
[15] M. Avram, I. G. Dinulescu, E. Manica, G. Mateescu, E. Sliam, and C. D. Nenitzescu, *Chem. Ber.*, 1964, **97**, 382.
[16] E. Eisenmann, Diplomarbeit, Freiburg, 1975.
[17] G. S. Hammond and C. D. De Boer, *J. Am. Chem. Soc.*, 1964, **86**, 899.
[18] M. J. Box, *The Computer J.*, 1965—1966, **8**, 42.
[19] H. M. Frey, H-D. Martin, and M. Hekman, *J. Chem. Soc., Chem. Commun.*, 1975, 204.
[20] E. N. Cain and R. K. Solly, *Int. J. Chem. Kinet.*, 1976, **8**, 563 and references therein.
[21] Ref. 2, p. 133.
[22] M. J. S. Dewar, S. Kirschner, H. W. Kollmar, and L. E. Wade, *J. Am. Chem. Soc.*, 1974, **96**, 5242.
[23] M. J. Goldstein and M. S. Benzon, *J. Am. Chem. Soc.*, 1972, **94**, 5119.
[24] J. E. Baldwin and P. W. Ford, *J. Am. Chem. Soc.*, 1969, **91**, 7192.
[25] A. T. Cocks, H. M. Frey, and I. D. R. Stevens, *Chem. Commun.*, 1969, 458.
[26] Ref. 2. ch. 3.
[27] G. Huybrechts, L. Luyckx, Th. Vandenboom, and B. Van Mele, *Int. J. Chem. Kinet.*, 1977, **9**, 283.
[28] M. P. Kozina, L. P. Timofeeva, G. L. Galčenko, E. A. Gvozdeva, and V. M. Cerednič enko, *Termodinamika Organisčeskich Soedinenij* (*Mežvuzovskij sbornik*), 1976, **5**, 9 (*Chem. Abs.* 1978, **89**, 5735).
[29] Estimate from ref. 2: data of ref. 30 are in poor agreement with this value and in our view less reliable.
[30] H-J. Rauh, W. Geyer, H. Schmidt, and G. Geiseler, *Z. Phys. Chem.* (*Leipzig*), 1973, **253**, 43.
[31] W. von E. Doering, M. Franck-Neumann, D. Hasselmann, and R. L. Kaye, *J. Am. Chem. Soc.*, 1972, **94**, 3833; and unpublished work on butadiene dimerization.
[32] A. A. Frost and R. G. Pearson, ' Kinetics and Mechanism ', Wiley, New York, 1961, 2nd edn., ch. 8, p. 160.
[33] Z. G. Szabo, ' Kinetic Characterisation of Complex Systems,' in ' Comprehensive Chemical Kinetics, Vol. 2. (The Theory of Kinetics) ' eds. C. H. Bamford and C. F. H. Tipper, Elsevier, London, 1969, p. 1.